NASA Technical Memorandum 87316

Turbulent Dispersion of the Icing Cloud From Spray Nozzles Used in Icing Tunnels

C. John Marek and William A. Olsen, Jr.
Lewis Research Center
Cleveland, Ohio

Prepared for the
Third International Workshop on Atmospheric Icing of Structures
Vancouver, Canada, May 6-8, 1986

NASA

TURBULENT DISPERSION OF THE ICING CLOUD FROM SPRAY NOZZLES USED IN ICING TUNNELS

John Marek and William A. Olsen, Jr.
National Aeronautics and Space Administration
Lewis Research Center
Cleveland, Ohio 44135

ABSTRACT

To correctly simulate flight in natural icing conditions, the turbulence in an icing simulator must be as low as possible. But some turbulence is required to mix the droplets from the spray nozzles and achieve an icing cloud of uniform liquid water content. The goal for any spray system is to obtain the widest possible spray cloud with the lowest possible turbulence in the test section of a icing tunnel.

This investigation reports the measurement of turbulence and the three-dimensional spread of the cloud from a single spray nozzle. The task was to determine how the air turbulence and cloud width are affected by spray bars of quite different drag coefficients, by changes in the turbulence upstream of the spray, the droplet size, and the atomizing air.

An ice accretion grid, located 6.3 m downstream of the single spray nozzle, was used to measure cloud spread. Both the spray bar and the grid were located in the constant velocity test section. Three spray bar shapes were tested: the short blunt spray bar used in the NASA Lewis Icing Research Tunnel, a thin 14.6 cm chord airfoil, and a 53 cm chord NACA 0012 airfoil.

At the low airspeed (56 km/hr) the ice accretion pattern was axisymmetric and was not affected by the shape of the spray bar. At the high airspeed (169 km/hr) the spread was 30 percent smaller than at the low airspeed. For the widest cloud the spray bars should be located as far upstream in the low velocity plenum of the icing tunnel.

Good comparison is obtained between the cloud spread data and predictions from a two-dimensional cloud mixing computer code using the two equation turbulence ($k\varepsilon g$) model.

Introduction

Refurbishment of the NASA Lewis Altitude Wind Tunnel (AWT), proposed for completion in the early 1990's, was planned to include the capability of conducting icing research along with aerodynamics, propulsion and acoustic studies. Since ice accumulation on aircraft and engine surfaces can seriously degrade performance, icing tests are an important aspect of the development and verification tests of aerospace flight systems. The ultimate goal of a ground based test facility is to effectively simulate actual icing conditions encountered by an aircraft in flight.

A spray bar and nozzle system is required to produce a uniform cloud. Consideration needs to be given to the spacing of the nozzles, the spacing of the spray bars, and the shape of the spray bars. Turbulence in an icing simulator must be as low as possible. But some turbulent mixing of the droplets from the spray nozzles is required to achieve an icing cloud of uniform liquid water content (LWC). Figure 1 shows a nozzle and a spray bar in a tunnel flow. The turbulence arises from three sources:

1. The air jet used to atomize the water into acceptably small droplets.
2. The wake of the spray bar.
3. The turbulent flow from upstream of the spray bars.

The goal of any icing simulator is to obtain the widest possible spray cloud for the lowest possible turbulence. The nozzles are spaced so that the sprays overlap to produce a fairly large uniform LWC.

The experience at the NASA Lewis Research Center in the Icing Research Tunnel (IRT) was with a short-chord blunt-trailing edge spray bar. The horizontal spray bars and spray nozzles of the IRT were developed in 1950. In the new AWT, low loss coefficient aerodynamic spray bars were proposed, it was expected that the large scale turbulence originating off the separated wake of the IRT spray bar would result in larger amounts of lateral mixing and was required to produce a wide dispersion of the spray. In addition spray dispersion data taken in the IRT showed a strong effect of the tunnel velocity on spread. The spread of the wake from an airfoil is not a function of the tunnel velocity, therefore, we wanted to study the spray/wake interaction.

The AWT was proposed to be a Mach 1 tunnel. It contains a six to one contraction to the test section so that for a given test section velocity, the velocity across the spray bars located upstream of the contraction is more than double that in the IRT tunnel with its 14:1 contraction. Because of the high velocities, the pressure loss across the spray bars was of concern, and it will be necessary to make them as streamlined as possible without adversely affecting the mixing of the spray.

The goals of this test were to: (1) examine the effect of spray bar shape on spray dispersion, (2) examine the effect of upstream turbulence on dispersion, and (3) compare the experimental results with numerical predictions of the cloud spread.

Three spray bar shapes were tested: the short (14.6 cm) blunt IRT spray bar, a thin 14.6 cm chord airfoil, and a 53 cm chord NACA 0012 airfoil. All spray bars were tested at airspeeds of 56 and 169 km/hr and two median volume droplet sizes, 12 and 22 μm. The IRT spray bars, upstream of the test section, were used to increase the upstream turbulence level by flowing air from the IRT spray nozzles. Longitudinal and transverse turbulence intensity measurements were made with single and cross hot wires, respectively.

Numerical Computer Model

To predict the dispersion of the spray a computer code which was developed for gas turbine combustors was used. The code had to take into account the effects of air turbulence on the spray dispersion. Many techniques exist in the literature, but the one used here was developed by Shuen, Solomon, Zhang, and Faeth (Ref. 1), and is based on the model of Gosman and Ioannides (Ref. 2). The model, called the

Stochastic Separated Flow (SSF) model, resulted in the best agreement with experimental data presented in Ref. 1.

Droplet trajectories were determined using a Lagrangian formulation of the governing equations. The droplet momentum equation is

$$\frac{dU_{pi}}{dt} = \frac{3\rho C_D}{4 d_p \rho_p} (U_i' - U_{pi}) \left| \overline{U} - \overline{U}_p \right| + g; \quad i=1, 3$$

where

C_D drag coefficient

g gravity

d_p droplet diameter

ρ_p droplet density

U_{pi} droplet velocity in ith direction

U_p total droplet velocity

ρ density of air

U_i' instantaneous air velocity in ith direction

$\overline{U}$ total air velocity

where the droplet motion is based on the instantaneous velocity of the continuous phase determined below from the turbulence properties.

Droplets were tracked through the airstream eddies in a stochastic manner, interacting with a single eddy for the shorter of two times - (1) the eddy life-time t_e and (2) the residence time t_p for the passage through the eddy. In the calculations presented here, two thousand droplets of a given size were tracked and statistically averaged to obtain the mean spray properties.

The mean turbulence was determined using the two equation turbulence ($k\varepsilon g$) model of Launder and Spalding, Ref. 3. The velocity u' of each eddy at the start of a droplet-eddy interaction was determined by choosing a Gaussian random number with a standard deviation of $(2k/3)^{1/2}$ and mean velocity U_i. The characteristic size L_e of an eddy is given as

$$L_e = C_\mu^{3/4} k^{3/2}/\varepsilon$$

where

k turbulent energy = $3/2\ U'^2$

ε turbulent dissipation

where $C_\mu = 0.09$. The eddy lifetime t_e is computed with

$$t_e = \frac{L_e}{\left(\frac{2k}{3}\right)^{1/2}}$$

The droplet residence time through an eddy is

$$t_p = \frac{L_e}{U_p}$$

where u_p is the droplet velocity. The droplet is assumed to interact with the same eddy as long as the time is less than t_e or t_p.

The gas phase velocity and turbulence levels were computed using the GENMIX computer program of (Ref. 5). Source terms were included to consider droplet-gas coupling using the droplet source in cell approach of (Ref. 6). A simpler model assuming constant turbulence properties was tried in this work but with unsatisfactory results. The interaction of the droplets with the atomizing air jet is important and is computed with the GENMIX program.

The assumed initial conditions were: a sonic velocity for the atomizing air for all pressures above the choked condition and a droplet velocity equal to the liquid exit velocity. The turbulence properties were taken to be those of case 2 from Ref. 1 which was for the exit conditions of a particle-laden tube.

Experimental Facility

The tests were conducted in the test section of the NASA Lewis IRT. The IRT is a closed loop refrigerated atmospheric total pressure wind tunnel. The test section is 1.83 m high and 2.75 m wide. The maximum test section velocity is 482 km/hr. Natural cloud conditions were simulated by an array of 77 air-atomizing nozzles located upstream of the contraction.

Cloud spread was established by measuring the ice shapes accreted on a pair of 0.32 by 2.54 by 75 cm bars mounted perpendicular to each other with the 0.32 cm edge facing into the flow. The ice thickness at each bar position after a period of time is directly proportional to the average cloud liquid water content at that cloud location.

The experimental configuration for the dispersion studies is shown in Fig. 2. The test spray bar was located at the start of the tunnel test section and the ice accretion crossbars were located at the end of the test section. In this way the spray cloud was located entirely within the test section so that the air velocity around the entire spray cloud was constant, and the air turbulence was at a minimum. At 169 km/hr the velocity across the spray bar was high enough to simulate the AWT spray bar velocity at the maximum proposed test section velocity.

The IRT spray bars, located 11 m upstream of the test section entrance, were used to increase the upstream air turbulence intensity by flowing air from the IRT spray nozzles. The ice accretion crossbars were located 6.32 m downstream of the single nozzle. This was the maximum distance downstream within the constant velocity section.

The crossbars were supported by a grid composed of 0.32 cm thick by 5.0 cm deep bars spaced 15.25 cm apart in both the horizontal and vertical directions. This grid was used for locating the center of the spray and for supporting the ice accretion cross made up of 0.32 cm thick by 2.54 cm deep bars. After an icing run the cross was removed and the ice accretion thickness measured at locations 2.54 cm apart along the vertical and horizontal directions.

After all of the icing tests were completed for each spray bar, the support grid was removed and the traversing aerodynamic probes were installed to measure the velocity and turbulence profiles across the center of nozzle jet. Measurements were made at

a tunnel temperature of 10 °C without water spray or heating of the atomization air. The traversing probes consisted of a total and static pressure probe, a thermocouple, a single hot wire and a cross hot wire to measure the axial and normal components of velocity. The first station was 0.6 m downstream of the nozzle and the probes were traversed horizontally. The second station was 5.81 m downstream of the nozzle. The traversing mechanism was manually moved between stations one and two after a test series.

A photograph of the thin 14.6 cm chord spray bar mounted in the tunnel is shown in Fig. 3. The thickness of this airfoil was 3.2 cm which was the smallest size that could contain the nozzle air, water and steam lines.

Photographs of all three spray bars are shown in Fig. 4. The NASA IRT spray bar was 7.62 cm thick with a chord length of 14.6 cm. It consisted of a shaped skin which was wrapped around the thin 14.6 cm airfoil. The shape of the IRT spray bar is shown in Fig. 1. The trailing edge was a quickly tapered 30° half-angle which resulted in flow separation. However the IRT spray bar does not cause strong backflow that would cause spray droplets to impinge upon the spray bar and freeze. None of the three spray bars tested caused ice to form on the spray bars. The NACA 0012 airfoil was chosen to have low aerodynamic drag and to have the same chord length as the proposed AWT spray bar design (53 cm).

The NASA Lewis standard icing spray nozzle is shown in Fig. 5. This nozzle produces a narrow spray angle of finely atomized droplets. The drop sizes reported were obtained from previous measurements taken with laser diagnostics. The atomizing air is introduced at a pressure above the choking condition for the exit orifice. The air leaves the nozzle and interacts with the water jet at sonic speeds. The atomizing air interacts both with the water spray and the tunnel air in the wake of the nozzle face to form a complicated flow configuration. The droplets breakup by going through the violence of a normal shock at the exit of the nozzle.

Results

Tests were completed to determine the spray dispersion width as a function of droplet size and tunnel velocity, and to evaluate the effect of the spray bar shape and turbulence on dispersion. The ice accretion on a grid was measured in order to determine the dispersion of the spray. Then the velocity and turbulence distribution were measured. Comparisons were made between numerical predictions of dispersion using a Monte Carlo model and the experimental data.

The ice accretion profiles for the IRT spray bar both along the spray bar (vertical) and normal to it (horizontal) are shown in Fig. 6 for a tunnel velocity of 56 km/hr. The spray pattern was axisymmetric so the distribution and spread are very close in both directions. The spray with the larger (22) median volume drop size did not disperse as much as the 12 μm droplets. The data have not been corrected for changes in catch efficiency because it should not affect the indicated spread of the cloud. The catch efficiency increases by 10 percent for the change from 12 to 22 μm drops.

The two airfoils also produced axisymmetric ice accretion patterns at the 56 km/hr tunnel velocity. The data for the three spray bars are shown in Fig. 7. At the low tunnel speed, the mixing is dominated by the atomization air and the shape of the spray bar does not influence the spreading. This result was surprising in that it was expected that the large scale turbulence orginating from the separated wake of the IRT spray bar would result in larger amounts of lateral mixing. The wide dispersion found in the IRT was thought to be produced by the blunt trailing edge of the IRT spray bar.

In Fig. 7(b) there appears to be a large difference in the centerline accretion level between the airfoils and the IRT spray bar, but the spray is not much wider for the IRT spray bar. Because of the circular pattern, differences in ice thickness at the larger radius greatly affects the centerline values. For example an increase of 0.5 mm at 30 cm would require a decrease of 1.5 mm at the center to maintain the same total mass of ice accreted.

At 169 km/hr the spray dispersion was greatly reduced. The ice accretion profiles for the 12 μm volume median drop size are shown in Fig. 8. The spray pattern for the IRT spray bar was elliptical but again not in the direction expected. At the higher velocity the spreading was greater along the IRT spray bar rather than in the normal direction indicating that the wake was producing a sheltered zone. The spreading along the IRT spray bar was the same as the lower velocity case. The spreading in the normal direction was nearly the same as the airfoils. The spray pattern for the airfoils appeared axisymmetric. The wake of the IRT configuration allowed increased spreading along the spray bar and did not increase the spreading normal to the spray bar. At a tunnel velocity of 169 km/hr the spreading was reduced in the normal direction by 30 percent from the lower velocity case for all three spray bars.

The 22 μm volume median drop size data are shown in Fig. 9. The curves are similar to the 12 μm data. The IRT spray bar curves are very elliptical. There is some variation in the peak levels between the NACA 0012 and the 14.6 cm airfoil. Some of the error is caused by the ice accretion cross not being exactly in the center of the pattern. For the steep gradients obtained, an error of 4 cm in position can produce a difference of 1 mm in ice accretion. The conclusions stated in the above paragraph apply to this data also.

Cloud spread was much wider at the low airspeed of these tests than at the high airspeed. Therefore for the widest cloud of uniform LWC and the lowest turbulence, spray bars should be located as far upstream as possible in the low velocity plenum chamber of an icing tunnel.

In order to determine the effect of upstream turbulence on spray dispersion, the IRT strut atomizing air was used which flowed out of 77 IRT nozzles upstream of the bellmouth. The ice accretion curves are shown in Fig. 10. The catch was reduced and more frost was produced outside the main area. The amount of frost produced, however, did not account for the decrease in catch. It is not known whether the increased turbulence affects the catch efficiency enough to alter the mass balance. The data for all the spray bar shapes produced similar results. The spread of the spray is not affected by the upstream turbulence. Some data at the higher velocity were taken but the reduction in catch was very high and is not presented.

Turbulence and velocity measurements were taken with a single and crossed hot wires. The probes at the 0.6 m position could be traversed out of the spray

bar wake to sample the upstream (freestream) conditions. The value of the turbulence is the RMS velocity divided by the local mean velocity. Figure 11 presents the effect of IRT strut air on tunnel turbulence. At 56 km/hr the upstream turbulence increased from 0.6 to 3.5 percent. At 169 km/hr the tunnel turbulence increased from 0.8 to 1.2 percent. The data from the single and cross wires agreed. The axial and vertical turbulence levels agreed well indicating that the fluctuations were nearly isotropic. A spectrum analysis of the signals indicated that no large waves were present.

At higher tunnel velocities the contribution of the strut air to the total turbulence was much lower. Assuming that the magnitude of the velocity fluctuations from the IRT strut air remains the same, increasing the velocity by a factor of three would decrease the turbulence intensity by the same factor. The effect of tunnel velocity on turbulence intensity is shown in Fig. 12. At a tunnel velocity of 300 km/hr the contribution of the atomizing air to the turbulence intensity is insignificant, but at low speeds (below 150 km/hr), the increase in turbulence could significantly affect the aerodynamic measurements. The difference in contraction ratio between the IRT and the proposed AWT tunnels would also affect the results.

Measurements of the velocity and turbulence at a distance 0.6 m downstream of the experimental IRT spray bar is shown in Fig. 13. This distance was chosen to be far enough away from the trailing edge to have pressure recovery of the flow. As the atomizing air pressure is increased, the wake of the spray bar is filled in the neighborhood of the nozzle, making the configuration a propelled body with a negative drag coefficient. It is interesting that the spread of the spray bar wake equals that of the atomizing air jet at this condition.

The wake turbulence level for the IRT spray bar is high with a peak of 13 percent. But with atomizing air the turbulence is dominated by the jet reaching a level of 20 percent for air pressures required for large drops and 45 percent for air pressures required for the small ones.

A comparison of velocity profiles and the turbulence distribution for the three spray bars is shown in Fig. 14. The velocity and turbulence profiles were much wider for the IRT spray bar. The wake turbulence was three times larger, which should result in greater mixing. The drag coefficient of the IRT spray bar was 18 times that of the NACA 0012 airfoil.

An unusual result was that the thin 14.6 cm airfoil produced a larger drag coefficient than the longer 53 cm NACA 0012 airfoil. Although the 14.6 cm airfoil was not separated, there was more flutter in the attached tufts indicating possible transition.

The turbulence measurements at 5.81 m are shown in Figs. 15 and 16 for the IRT and NACA 0012 spray bar shapes respectively. No velocity data are presented because a significant velocity difference in the wake was not seen at this axial position. At low velocity for the IRT spray bar with no atomizing air the turbulence wake appears almost doubly humped. As the atomizing air is increased the dominance of the jet is seen. Surprizingly at 169 km/hr velocity, the atomizing air jet was dissipated by 5.81 m and the profiles are nearly identical. This occurred for both spray bars.

The interaction of droplets with a turbulent airstream is very complex which emphasizes the need for a numerical model. The numerical results have been plotted along with the experimental data for the 56 km/hr velocity on Fig. 17. The agreement with the experimental data is good for both droplet sizes. The numerical predictions have been normalized by the peak of the experimental curve. In the numerical calculations only a single dropsize was used, whereas in the experimental data the spray contains a wide range of drop sizes. All three spray bar shapes gave the same dispersion at low velocities so that the spreading was governed by the atomization air. No attempt was made to adjust the initial conditions to determine the sensitivity of the results. The measurement station was located 1975 nozzle diameters downstream of the nozzle exit. Because the GENMIX code is a forward marching (parabolic) code, it could not handle the recirculation zones behind the IRT spray bar. The calculations were performed assuming a positive freestream velocity with a 5 percent turbulence level.

The comparison between the numerical results and the experimental data at 169 km/hr is shown in Fig. 18. The numerical results agree very well with the data for the airfoils. Again the numerical predictions were normalized this time by a value between the peaks of the airfoils. Reduction in the profile for the IRT spray bar was a three-dimensional effect and because the code was two-dimensional, it was not able to predict this. The numerical code does predict the collapse of the spray with increased tunnel velocity. This effect is computed for a jet in Abramovich, Ref. 6.

Conclusions:

1. Cloud spread was much wider at the low airspeed of these tests than at the high airspeed. Therefore for the widest cloud of uniform liquid water content (LWC) and the lowest turbulence, spray bars should be located as far upstream as possible in the low velocity plenum chamber of the icing tunnel.

2. At the low airspeed (56 km/hr) the ice accretion pattern (i.e., cloud spread) from the single nozzle was axisymmetric and not affected by the shape of the spray bar. This result was true for the 12 and 22 μm droplet spray tests. The dispersion was dominated by the atomizing air jet.

3. At the high airspeed (169 km/hr) the ice accretion pattern was not axisymmetric. The cloud spread more along the spray bar than perpendicular to it. Furthermore, the cloud spread along the IRT spray bar which is blunt with a high drag coefficient, was much broader than along the low drag spray bars. These results were true for both droplet sizes tested. This does not impact the IRT tunnel operation because the maximum airspeed at the spray bars is only 35 km/hr.

4. At the low airspeed, the upstream turbulence could be increased from 0.5 to 3.5 percent by turning on the air to the IRT spray bars. In spite of this large increase, the cloud spread did not change noticeably. The catch however was reduced. This demonstrates that the turbulence generated upstream was not important to mixing.

5. Upstream turbulence did not affect the cloud spread.

6. The predictions of the stochastic separated flow (SSF) computer model compared well with the experimental data.

REFERENCES

1. Shuen, J.S., et al: A Theoretical and Experimental Study of Turbulent Particle-Laden Jets, NASA CR-168293, November 1983.

2. Gosman, A.D.; and Ioannides, E.: Aspects of Computer Simulation of Liquid-fueled Combustors. J. Energy, vol. 7, no. 6, Nov.-Dec. 1983, pp. 482-490.

3. Launder, B.E.; and Spalding, D.B.: Mathematical Models of Turbulence. Academic Press, 1972.

4. Pantankar, S.V.; and Spalding, D.B.: Heat and Mass Transfer in Boundary Layers. 2nd ed., International Textbook Company, London, 1970.

5. Crowe, C.T.; Sharma, M.P.; and Stock, D.E.: The Particle-Source-in Cell (PSI-CELL) Model for Gas-Droplet Flows. J. Fluids Eng., vol 99, no. 2, June 1977, pp. 325-332.

6. Abramovich, G.N.: The Theory of Turbulent Jets. MIT Press, 1963.

7. Boldman, D.: Personal Communication, NASA Lewis Research Center, 1985.

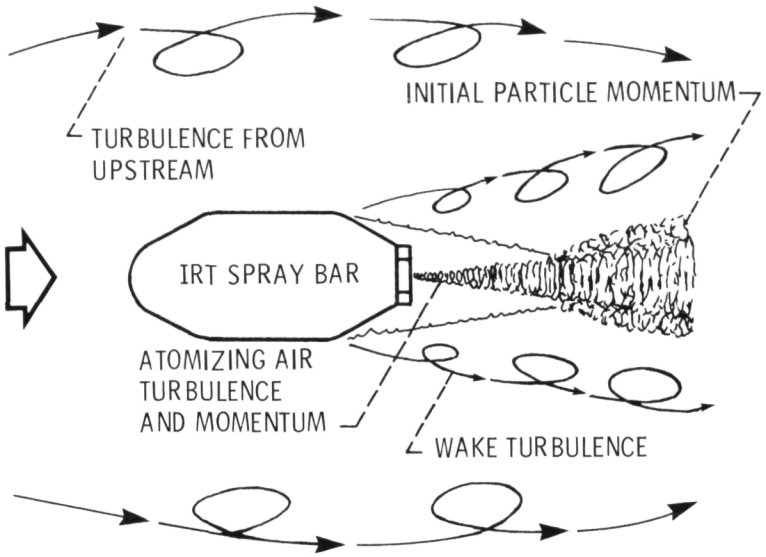

Figure 1. - Flowfield-droplet interactions to consider.

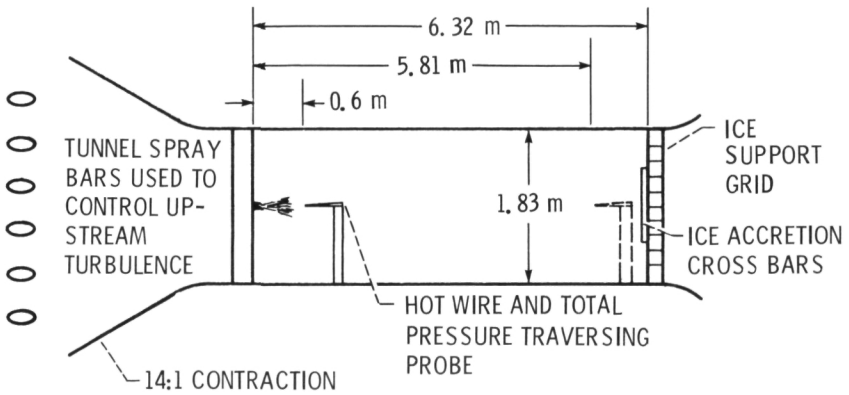

Figure 2. - IRT Tunnel with single nozzle mounted in test section and ice accretion grid. Tunnel is 1.83 m by 2.75 m.

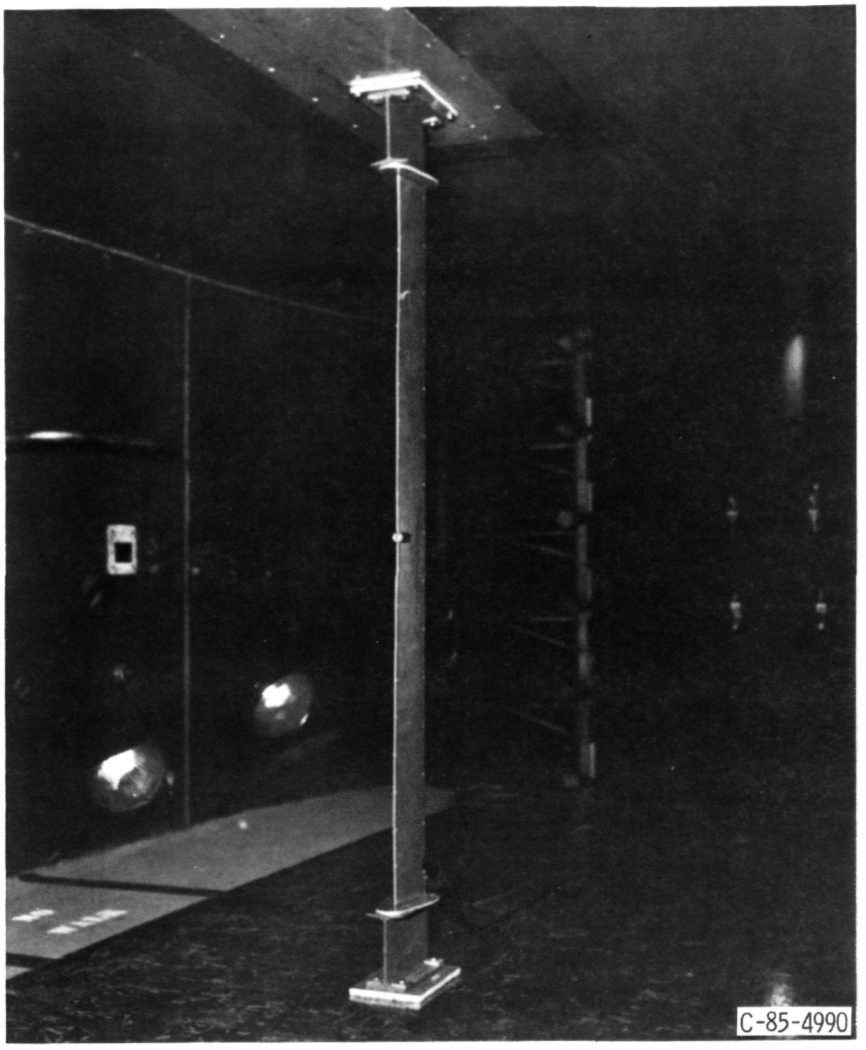

Figure 3. - Photograph of airfoil mounted in tunnel looking upstream.

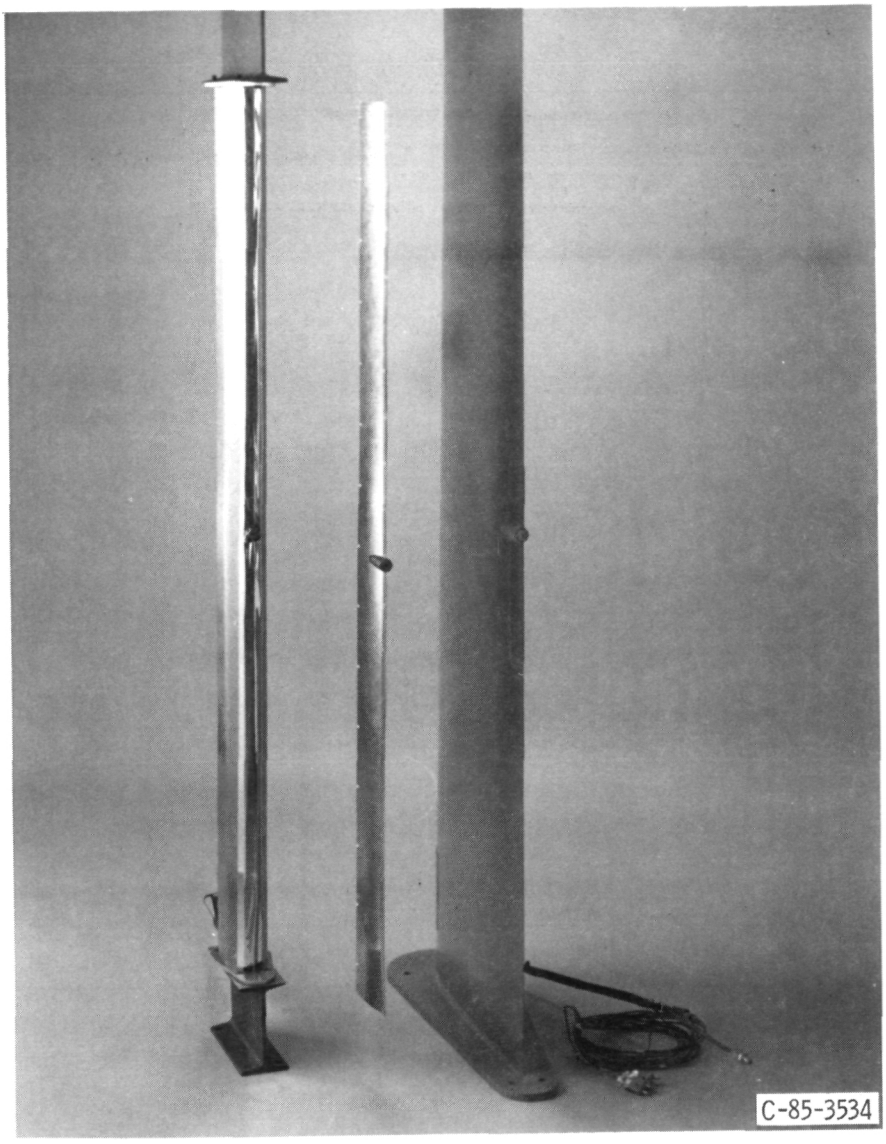

Figure 4. - Photograph of the three airfoils tested - IRT, 0.146 meter, and the NACA 0012.

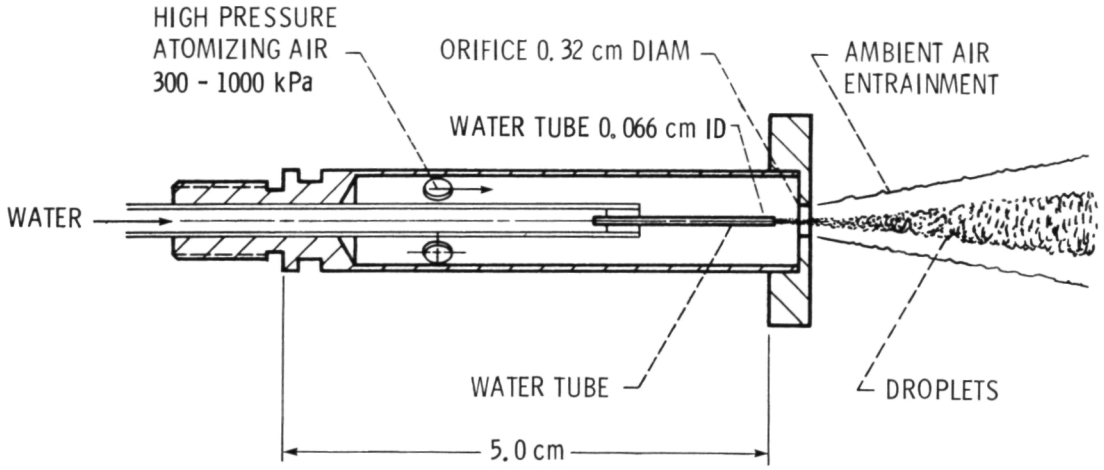

Figure 5. - NASA - Lewis standard icing spray nozzle.

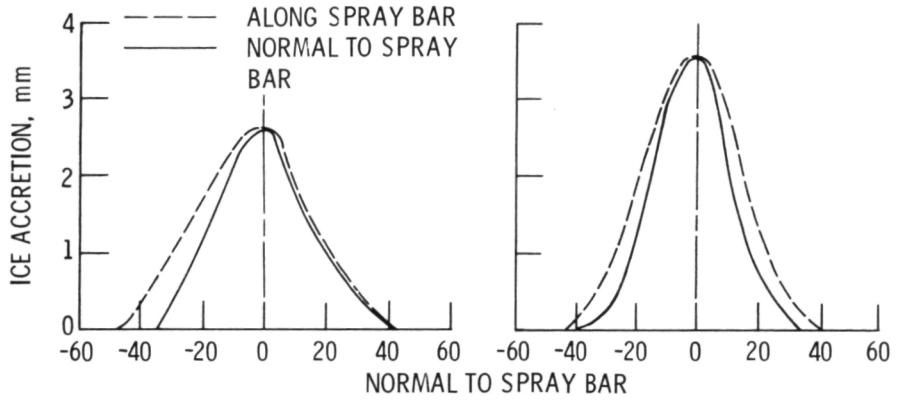

(a) 12 Micrometers dropsize. (b) 22 Micrometers dropsize.

Figure 6. - Spray dispersion from IRT spray bar at 56 km/hr. Tunnel temperature, -13 ^{o}C; 3 min. sprays.

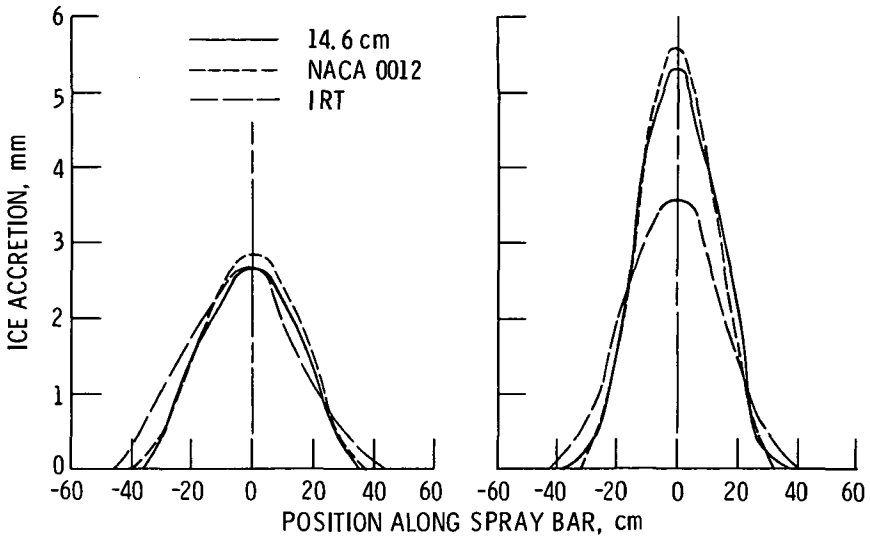

(a) 12 Micrometers droplet size. (b) 22 Micrometer droplet size.

Figure 7. - Comparison of spray dispersion from three spray bars at 56 km/hr Tunnel temperature, -13 °C; 3 min. sprays.

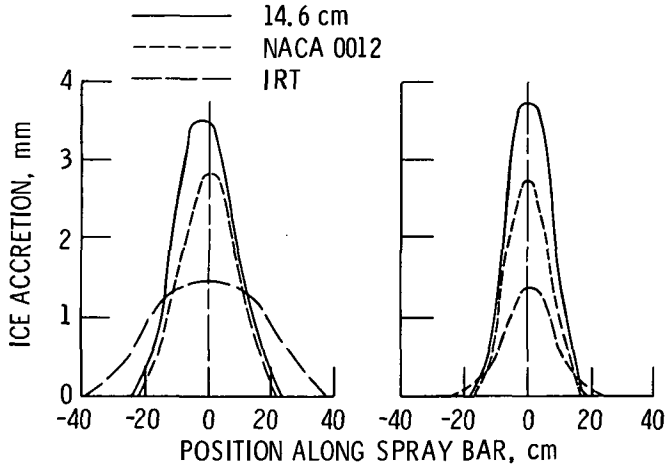

Figure 8. - Comparison of spray dispersion from 3 spray bars at 169 km/hr. Drop size, -12 μm; tunnel temperature, -13 °C; 1-min sprays.

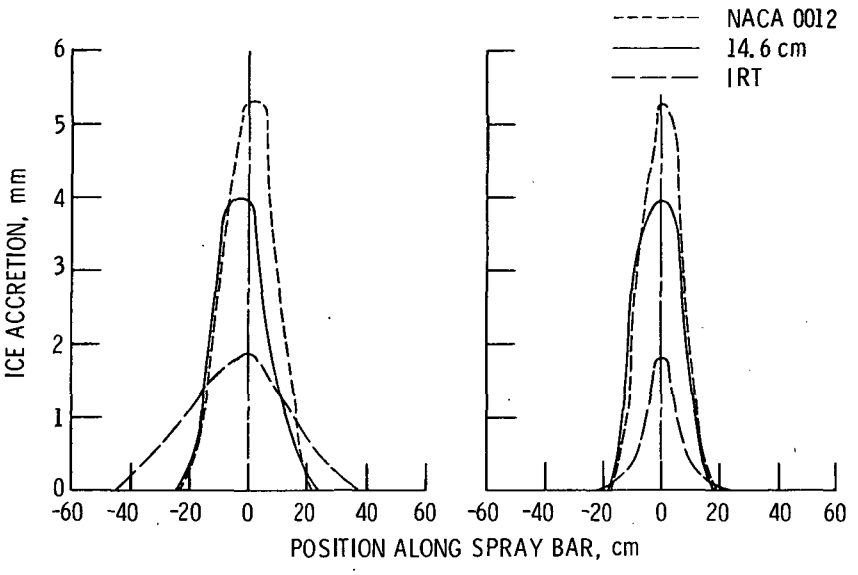

Figure 9. - Comparison of spray dispersion from 3 spray bars at 169 km/hr drop size, -22 μm, tunnel temperature, -13 °C; 1-min sprays.

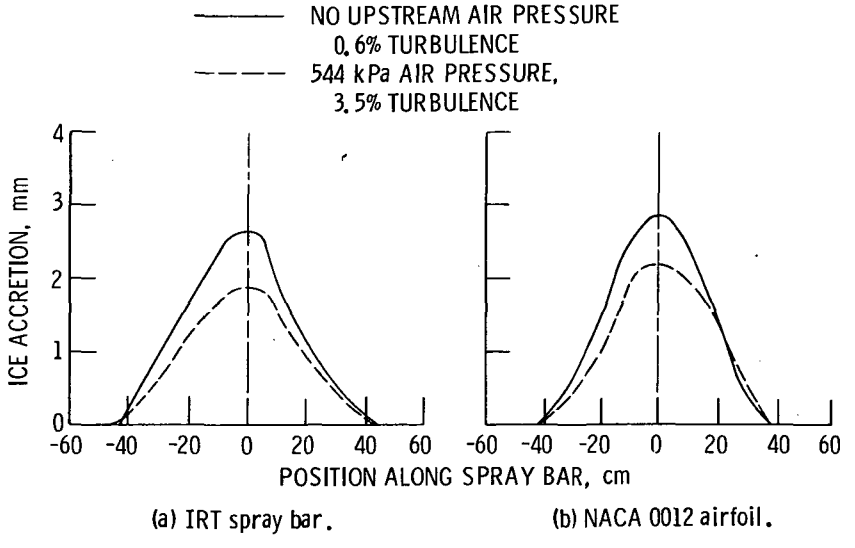

(a) IRT spray bar. (b) NACA 0012 airfoil.

Figure 10. - Effect of upstream turbulence on spray dispersion at 56 km/hr. Dropsize - 12 micrometers. Tunnel temperature, -13 °C, 3 min. sprays.

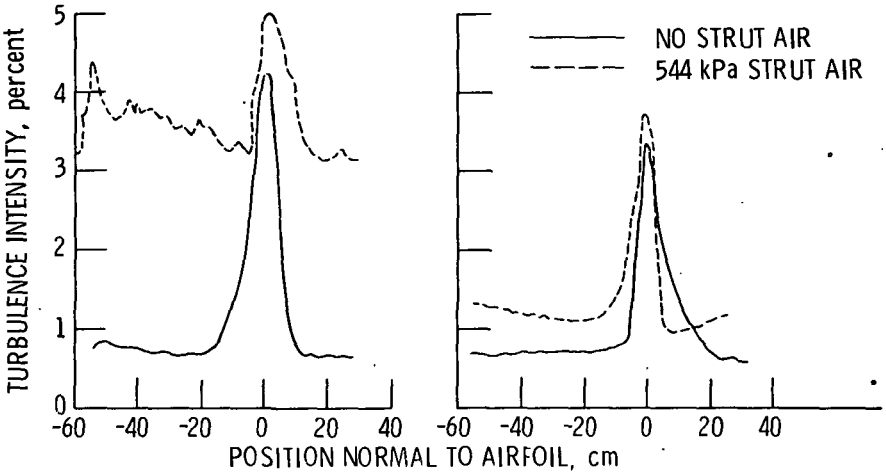

(a) Tunnel velocity, 56 km/hr. (b) Tunnel velocity, 169 km/hr.

Figure 11. - Effect of upstream spray bar flow on tunnel turbulence at 0.6 m downstream of NACA 0012 airfoil.

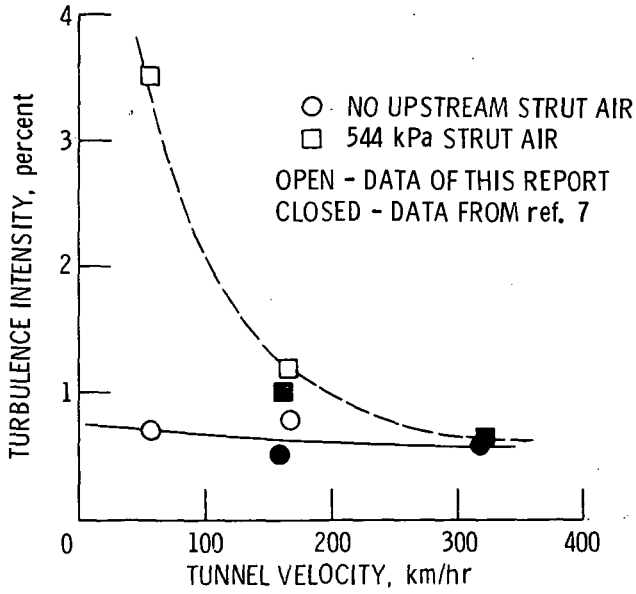

Figure 12. - Test section turbulence.

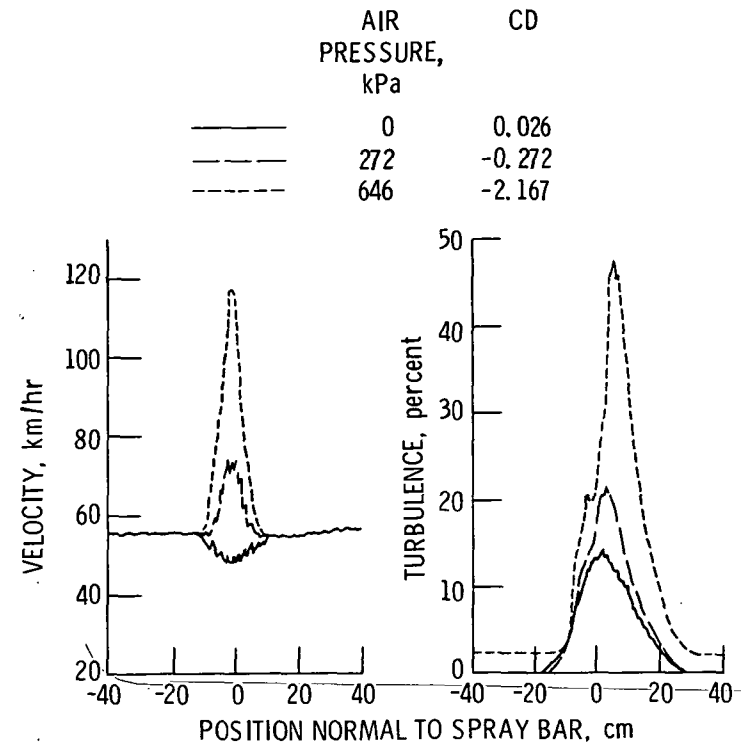

Figure 13. - Effect of nozzle air pressure for IRT spray bar at 0.6 m downstream of trailing edge at 56 km/hr.

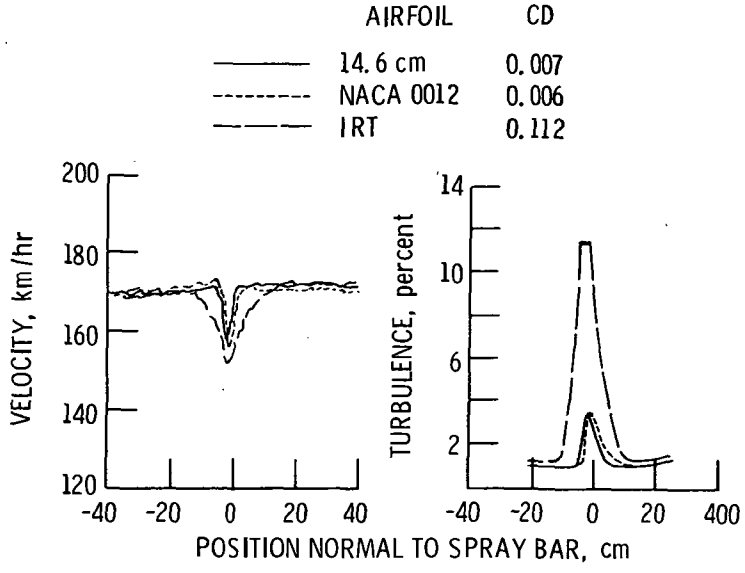

Figure 14. - Effect of airfoil shape on tunnel flow 0.6 m downstream of the trailing edge, 169 km/hr - no nozzle air pressure.

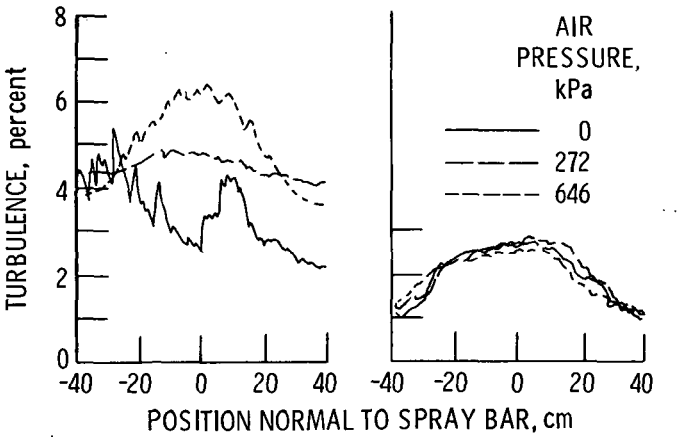

(a) Tunnel velocity, 56 km/hr.

(b) Tunnel velocity, 169 km/hr.

Figure 15. - Effect of nozzle air pressure on turbulence for IRT spray bar at 5.81 m downstream.

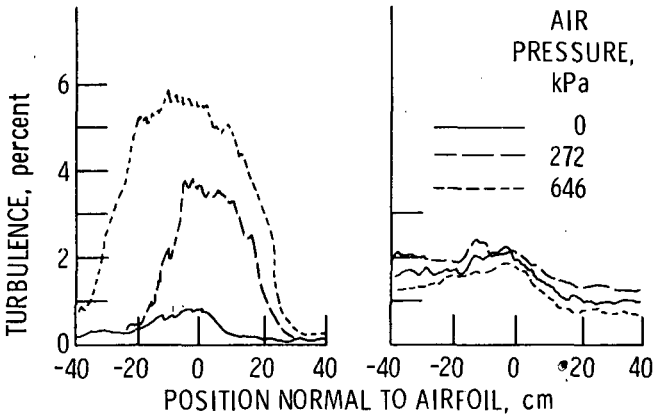

(a) Tunnel velocity, 56 km/hr.

(b) Tunnel velocity, 169 km/hr.

Figure 16. - Effect of nozzle air pressure on turbulence for NACA 0012 airfoil at 5.81 m downstream of the trailing edge.

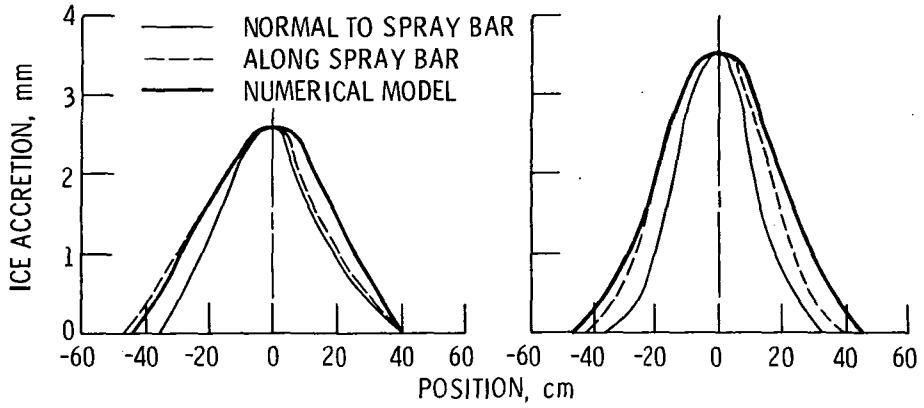

(a) 12 Microns diameter. (b) 22 Microns diameter.

Figure 17. - Comparison of numerical model with experimental spray dispersion for IRT spray bar at 56 km/hr. Tunnel temperature, -13^{0}C, 3-min sprays.

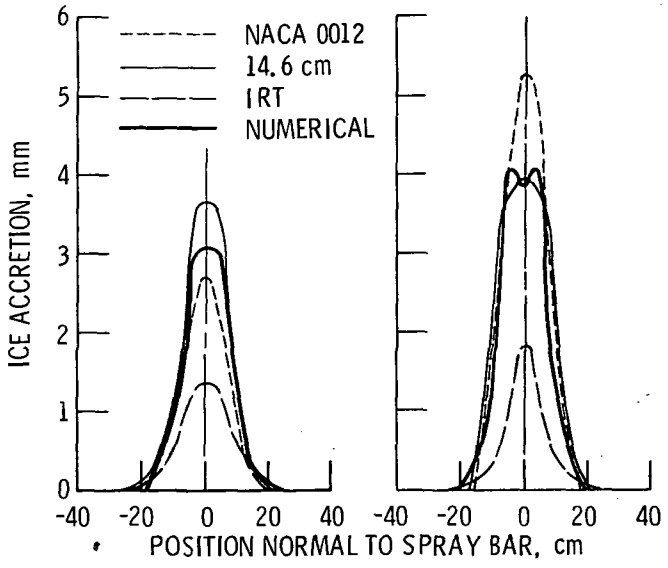

(a) 12 Micrometers drop size. (b) 22 Micrometers drop size.

Figure 18. - Comparison of numerical results with experimental data at 169 km/hr.

1. Report No.	2. Government Accession No.	3. Recipient's Catalog No.
NASA TM-87316		

4. Title and Subtitle	5. Report Date
Turbulent Dispersion of the Icing Cloud From Spray Nozzles Used in Icing Tunnels	6. Performing Organization Code: None

7. Author(s)	8. Performing Organization Report No.
C. John Marek and William A. Olsen, Jr.	E-3047
	10. Work Unit No.

9. Performing Organization Name and Address	11. Contract or Grant No.
National Aeronautics and Space Administration Lewis Research Center Cleveland, Ohio 44135	13. Type of Report and Period Covered: Technical Memorandum

12. Sponsoring Agency Name and Address	14. Sponsoring Agency Code
National Aeronautics and Space Administration Washington, D.C. 20546	

15. Supplementary Notes

Prepared for the Third International Workshop on Atmospheric Icing of Structures, Vancouver, Canada, May 6-8, 1986.

16. Abstract

To correctly simulate flight in natural icing conditions, the turbulence in an icing simulator must be as low as possible. But some turbulence is required to mix the droplets from the spray nozzles and achieve an icing cloud of uniform liquid water content. The goal for any spray system is to obtain the widest possible spray cloud with the lowest possible turbulence in the test section of a icing tunnel. This investigation reports the measurement of turbulence and the three-dimensional spread of the cloud from a single spray nozzle. The task was to determine how the air turbulence and cloud width are affected by spray bars of quite different drag coefficients, by changes in the turbulence upstream of the spray, the droplet size, and the atomizing air. An ice accretion grid, located 6.3 m downstream of the single spray nozzle, was used to measure cloud spread. Both the spray bar and the grid were located in the constant velocity test section. Three spray bar shapes were tested: the short blunt spray bar used in the NASA Lewis Icing Research Tunnel, a thin 14.6 cm chord airfoil, and a 53 cm chord NACA 0012 airfoil. At the low airspeed (56 km/hr) the ice accretion pattern was axisymmetric and was not affected by the shape of the spray bar. At the high airspeed (169 km/hr) the spread was 30 percent smaller than at the low airspeed. For the widest cloud the spray bars should be located as far upstream in the low velocity plenum of the icing tunnel. Good comparison is obtained between the cloud spread data and predictions from a two-dimensional cloud mixing computer code using the two equation turbulence ($k\varepsilon g$) model.

17. Key Words (Suggested by Author(s))	18. Distribution Statement
Sprays Dispersion Turbulence Modeling	Unclassified - unlimited STAR Category 07

19. Security Classif. (of this report)	20. Security Classif. (of this page)	21. No. of pages	22. Price*
Unclassified	Unclassified		

*For sale by the National Technical Information Service, Springfield, Virginia 22161